



UNIVERSITY OF LEEDS

This is a repository copy of *Characterization of boron nitride nanosheets synthesized by boron-ammonia reaction*.

White Rose Research Online URL for this paper:

<https://eprints.whiterose.ac.uk/160742/>

Version: Accepted Version

Article:

Nadeem, A, Raza, MA, Maqsood, MF et al. (3 more authors) (2020) Characterization of boron nitride nanosheets synthesized by boron-ammonia reaction. *Ceramics International*, 46 (12). pp. 20415-20422. ISSN 0272-8842

<https://doi.org/10.1016/j.ceramint.2020.05.132>

© 2020 Elsevier Ltd and Techna Group S.r.l. All rights reserved. This manuscript version is made available under the CC-BY-NC-ND 4.0 license
<http://creativecommons.org/licenses/by-nc-nd/4.0/>

Reuse

This article is distributed under the terms of the Creative Commons Attribution-NonCommercial-NoDerivs (CC BY-NC-ND) licence. This licence only allows you to download this work and share it with others as long as you credit the authors, but you can't change the article in any way or use it commercially. More information and the full terms of the licence here: <https://creativecommons.org/licenses/>

Takedown

If you consider content in White Rose Research Online to be in breach of UK law, please notify us by emailing eprints@whiterose.ac.uk including the URL of the record and the reason for the withdrawal request.



eprints@whiterose.ac.uk
<https://eprints.whiterose.ac.uk/>

Characterization of boron nitride nanosheets synthesized by boron-ammonia reaction

¹Aamir Nadeem, *¹Mohsin Ali Raza, ¹Muhammad Faheem Maqsood, ¹Muhammad Tasaduq Ilyas, ²Aidan Westwood, ¹Zaeem Ur Rehman

¹Department of Metallurgy and Materials Engineering, Faculty of Engineering and Technology, University of the Punjab, Lahore, Pakistan

²School of Process and Chemical Engineering, University of Leeds, LS2 9JT, Leeds, UK

*Email of corresponding author: mohsin.ceet@pu.edu.pk

Abstract

Boron nitride nanosheets (BNNS) with thickness 5-11 nm were successfully produced when pure boron powder (1-2 μm) interacted with ammonia gas in chemical vapour deposition set up. Under the optimized parameters, at 1200 °C and for uninterrupted one hour of reaction duration, 2D BNNS with thickness of ca.11 nm were synthesized. BNNS were characterized by X-ray diffraction (XRD) for crystal structure, scanning electron microscopy for dimensions and morphology, energy dispersive X-ray analysis for chemical composition and Fourier transform infrared spectroscopy for sp^2 BN bond detection. The thickness of BNNS determined from both XRD data (using Scherrer equation) and atomic force microscopic analysis confirmed the stated product thickness. The BNNS obtained at 1200 °C had high crystallinity, purity and yield.

Keywords

Boron nitride nanosheets; Chemical vapour deposition; X-ray diffraction; Scanning electron microscopy; Atomic force microscopy

1. Introduction

Two-dimensional (2D) nanomaterials (graphene and boron nitride nanosheets (BNNS), metal dichalcogenides) have triggered tremendous research interests due to their outstanding properties such as exceptional electronic transport [1-3], large specific surface area, extraordinary optical transparency, mechanical properties and thermal conductivity [4, 5]. Due to these properties, 2D nanomaterials have become potential candidates for various applications in electronics [6], optoelectronics [7], catalysts [8], energy storage devices [9], sensors [10], solar cells [11], lithium batteries [12] and composites [13] etc.

Similar to various nanoforms of graphite, BN nanoforms also have gained attraction of both academia and industry [14]. BNNS and boron nitride nanotubes (BNNTs) are two nano derivatives of BN which are analogous to graphene nanoplatelets and carbon nanotubes, respectively [15]. Unlike carbon nanomaterials, BN nanomaterials are electrically insulating and have excellent dielectric properties [16]. BNNS is one of the interesting nanoforms of BN which resembles graphene nanosheets, also called “white graphene” [17]. BNNS has 2D morphology like graphene and may have thickness 0.35-100 nm. Like graphene, BNNSs are impermeable, have excellent mechanical properties and thermal conductivity [14, 16, 18], however, their high thermal stability, oxidation resistance and good dielectric properties make them different from graphene, which enable their use for such applications where graphene cannot be used [19]. In recent year, several articles published on BNNS highlighted that these can be beneficial for various applications. For example, their insulating nature can be beneficial for dielectric applications (dielectric gate layer) [20] and as ultraviolet (UV) luminescent material [7]. The thermal conductivity of BNNS is 1700-2000 W/mK [21], which makes them an ideal material for thermal interface applications [22]. The bending modulus of BNNS was found to be 18-32 GPa [15, 23]. Owing to its superior mechanical properties, BNNS can be a suitable nanofiller for improving mechanical properties of composite materials [13, 24]. The promising potential of BNNS is being reported successful for many sought after industrial applications such as water-repelling [25], anti-fouling [26], self-cleaning [27], anti-corrosion system [28] and solid-state lubricants [29].

Economic bulk manufacturing of few layered BNNS with acceptable purity is not less than a challenge. In literature, many methods are reported for the production of BNNS such as

chemical/liquid exfoliation [13], mechanical cleavage [30], selective etching [31], wet-chemical synthesis [14], high-energy electron beam [32] and chemical vapor deposition (CVD) [26]. A brief overview of BNNS' synthesis methods is presented here. Liquid exfoliation is a simple method based on top-down approach in which BNNS are produced by breaking the interlayer cohesion of bulk h-BN precursor in various solvents. Zhi et al. [13] produced BNNS by sonicating BN micron-sized particles in N-dimethyl formamide solvent using probe-type sonicator for 10 h. The resulting BNNS had thickness of 1-5 nm, which were comparable to few layered graphene. Wang et al. [33] produced BNNS with thickness of 2 nm by exfoliating micron-sized BN in methane sulphonic acid for 8 h using ultra-sonication. In an another study, Marsh et al. [34] produced BNNS with thickness ranging from 7-9 nm by sonicating bulk BN in tert-butanol 60 wt/wt. % in water. Thangasamy and Sathish [35] reported synthesis of BNNS by sonicating BN powder in isopropanol-water mixture (1:1 vol.%) for 5 min. The resulting solution was poured into stainless steel reactor vessel which was heated in furnace at 400 °C for 15 min and then was quenched in ice-cold water. The exfoliated solution was centrifuged to separate BNNS. Liquid exfoliation methods are more suitable for economical and large scale production of BNNS. However, yield of these methods is much less which is considered to be a major hindrance for the scalability of these processes.

CVD, a high temperature process based on bottom-up approach requires boron rich precursors such as boron oxide, ammonia borane, borazine or diborane which upon decomposition and reaction with nitrogen at high temperature produces BN. Gao et al. [36] synthesized BNNS having 25-50 nm thickness from mechanically mixed precursors, B₂O₃ and melamine powder, in CVD furnace at 1100-1350 °C for 1 hour in the flow of Argon (Ar) and Nitrogen (N₂) gases. Nag et al. [14] synthesized BNNS in CVD furnace at 900 °C for 5 hours in N₂ atmosphere using boric acid and urea as precursor with different molar ratios of dried precursors. They found BNNS thickness of 0.4-5 nm by AFM, and this was learnt that by changing the molar ratios of boric acid and urea, the thickness of BNNS also changed. CVD method has more potential for scalability as BNNS with high yield can be produced. However, the precursors reported for the production of BNNS are extremely expensive, which perhaps is the main limitation of the CVD process.

Nitridation of glasses is well established technique to improve physical and mechanical properties of the glasses [37-40]. In this technique glass is treated with either nitrogen or

ammonia gas at an appropriate temperature. The similar strategy is adopted in this work in which boron powder is nitrided by ammonia gas. This research work reports a novel approach of synthesis of BNNS from the direct reaction of pure boron powder with ammonia gas in a CVD furnace. Previously, mechanisms of the reactions of a boron atom with ammonia were studied computationally using hybrid density functional theory by Wang et al. [41]. However, to the best of our knowledge BNNS synthesis from boron and ammonia reaction has not been reported yet. The advantage of our method is that no expensive boron precursors or gases are used. We studied and controlled two parameters temperature and time of reaction in CVD furnace to find optimum parameters for the production of high quality BNNS with high yield. The resulting BNNS are characterized for their structure, morphology and chemical composition using various techniques.

2. Materials and methods

2.1. Material

Boron powder was purchased from US Research Nanomaterials, Inc. having particle size 1-2 μm and a purity of 99 %. Ammonia gas was obtained from the local industry.

2.2. BNNS production

A series of experiments were designed with two important parameters temperature and reaction time varying from 900 to 1400 $^{\circ}\text{C}$ and 1 to 9 hours, respectively. Each experiment had the similar procedure. Briefly, 100 mg of boron powder (precursor) was taken in an alumina boat which was placed in the quartz tube for heating in CVD furnace. The CVD furnace chamber was degassed by applying vacuum for 30 minutes. After complete degassing, ammonia gas was allowed to pass through the quartz tube (500 sccm) at room temperature. Then the furnace temperature was increased to desired level (900 to 1400 $^{\circ}\text{C}$) at a heating rate of 50 $^{\circ}\text{C}/\text{min}$. Once the set temperature was achieved, the reaction time varied from 1 to 9 hours in a series of experiments. After completion of a reaction time, furnace was switched off and the product was allowed to anneal in the presence of ammonia gas which was kept present in the quartz tube after closing the valves on either sides of the tube. Upon cooling, product of the reaction was taken

out and weighed. Ammonia flow was maintained constant for all the experiments. A schematic of CVD apparatus is shown in Fig. 1.

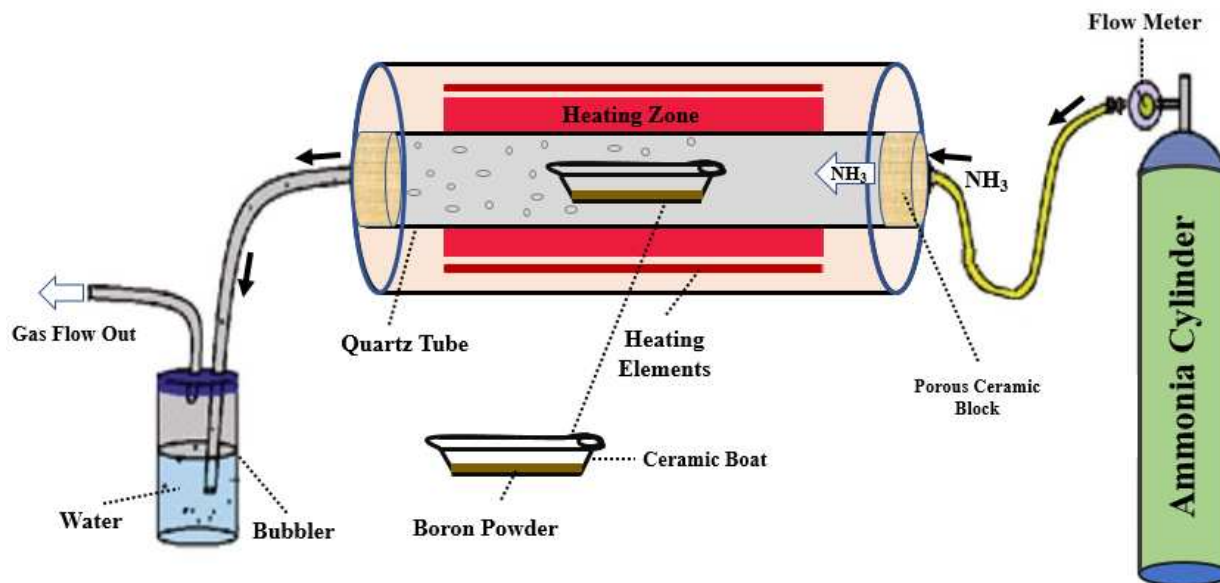


Fig. 1. Schematic of CVD apparatus used in this study

2.3. Characterization

The resultant product of the boron and ammonia reaction was characterized by selected techniques. For crystal structure of BNNS, X-ray diffraction was performed in a diffractometer (Equinox 2000, Thermo Scientific, USA) equipped with a curved position sensitive detector. Powder samples were filled in reflection-mode sampling cups which were placed on a spinning stage. The data was obtained in a real time in the range of $2\theta=2-116^\circ$ using $\text{CuK}\alpha 1$ radiation (0.15406 nm) obtained using germanium monochromator. The data acquisition time was 3-5 min. The data was analyzed using Match softwareTM and COD reference database. The thickness of BNNS was determined using Scherrer equation by considering broadening of (002) peak of BNNS [42] for which a commercial micron-sized BN was used as a standard sample. Scanning electron microscopy (SEM, [Nova NanoSEM 450, FEG-SEM, FEI, Thermo Scientific, USA]) was performed to determine morphology of the BNNS. Samples were sputter coated with gold prior to SEM analysis. Energy dispersive X-ray analysis (EDX) was performed to determine chemical composition of BNNS developed. It was carried out with EDAX system (Ametek, Inc.

Materials Analysis Division, USA) consisting of solid state silicon drift detector (silicon nitride window with diameter of 25 mm²) using TEAMTM software. B-N bond formation in the resultant CVD product was confirmed using Fourier Transform infrared spectroscopy (FTIR) which was performed using ATR mode FTIR spectrometer (Shimadzu, Japan). BNNS lateral dimensions and thickness was determined by atomic force microscopy (AFM). AFM was carried out in semi-contact mode (Nano-Solver, NT-MDT, Russia) on sheets which were deposited on mica substrate by spin coating dispersion of BNNS/ethanol followed by evaporation of solvent. The dispersion was prepared by dispersing 5 mg of the BNNS in 20 ml of ethanol using probe sonication (Soniprep 150, MSE, UK) for 2 h. Band gap of BNNS was determined using UV-Vis spectroscopy (Spectro-115U, Reference 3000, Gamry Instruments, USA) on the suspension of BNNS which were sonicated in blank soln. (DI water).

3. Results and discussion

3.1. XRD

XRD patterns of BNNS synthesized at 900 °C for 1 to 9 h of successive experimentation are presented in Fig. 2 (a). A broad peak at $2\theta = 26.78^\circ$ can be seen in all the patterns. This peak is similar to (002) peak of h-BN (COD Entry # 96-101-0603). The broader peak in Fig. 2 (a) suggests BNNS are turbostratic (partially crystalline) and have layers which are stacked roughly parallel to each other but have some random rotation and translation about the layer normal. Similar structure was reported by Thomas et al. [43] and Gross et al. [44]. However, peaks marked with asterisk in Fig. 2 are of boron which remained unreacted during the reaction at 900 °C. This suggests that BNNS formed at 900 °C for all the reaction times studied in this work were impure. The thickness of BNNS produced at 900 °C determined by Scherrer equation was found to be ca. 5 and 6 nm after 1 and 9 h of reactions time, respectively (Table 1).

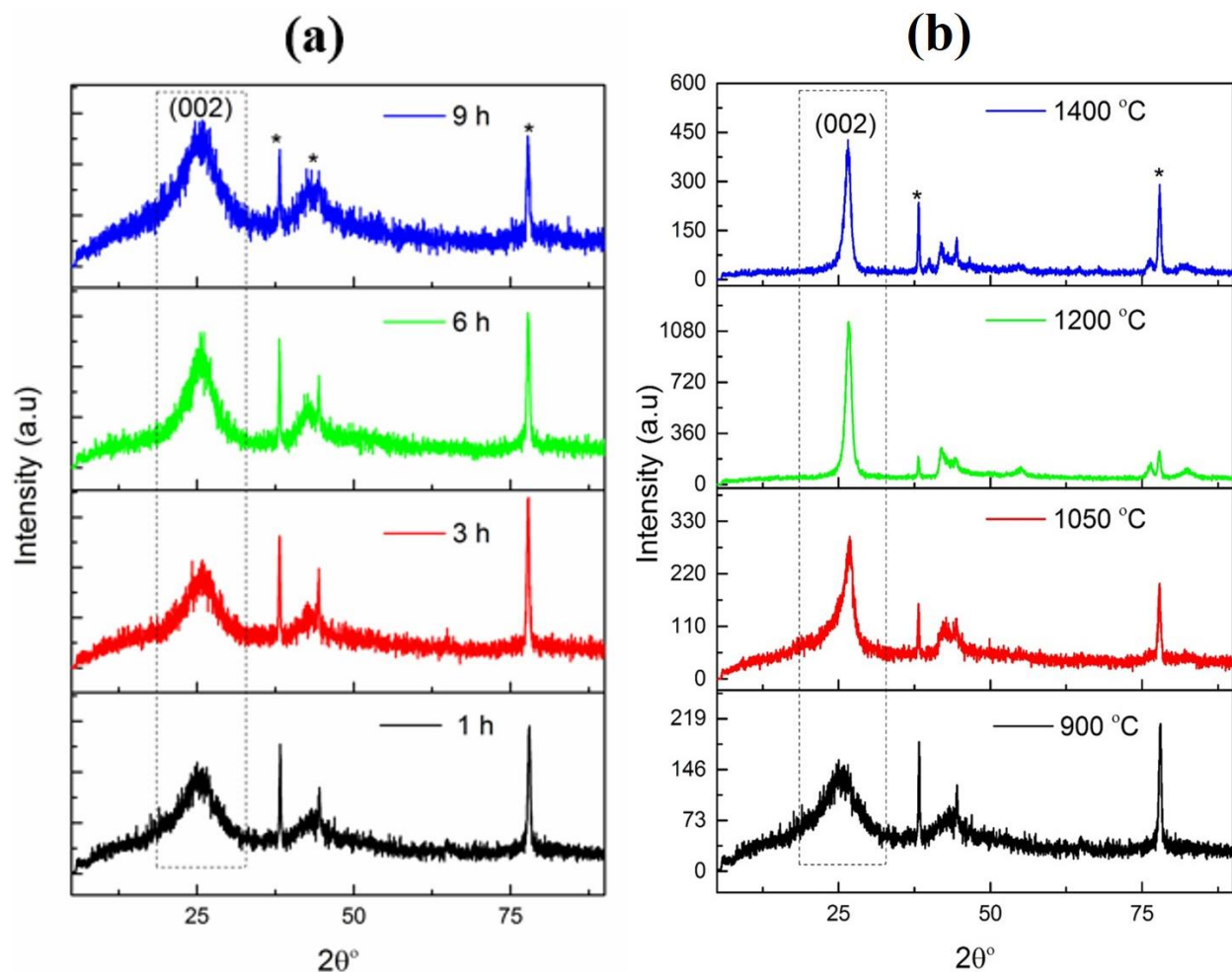


Fig. 2. XRD pattern of BNNS synthesized at (a) 900 °C for different times (b) different temperatures for 1 h

Fig. 2(b) presents comparison of the XRD patterns of BNNS synthesized at different temperatures and a constant reaction time of 1 h. It is noticeable that with the increasing temperature intensity of (002) peak increased suggesting good crystallization of BNNS in the resulting product. The peaks marked with asterisk in Fig. 2(b) also decreased with increase of temperature from 900 to 1200 °C, and at 1400 °C these peaks started to rise again. These peaks basically are due to unreacted boron left in the CVD product. XRD pattern of boron is shown in Fig.3 (b) which has these peaks as the prominent ones. Thus, 1200 °C seems to be an optimum temperature at which BNNS can be synthesized with high crystallinity, high purity and high yield. The colour of the product obtained at 1200 °C and 1 h was also milky white. The thickness of BNNS as determined by Scherrer equation was found to be ca. 11 nm (Table 1).

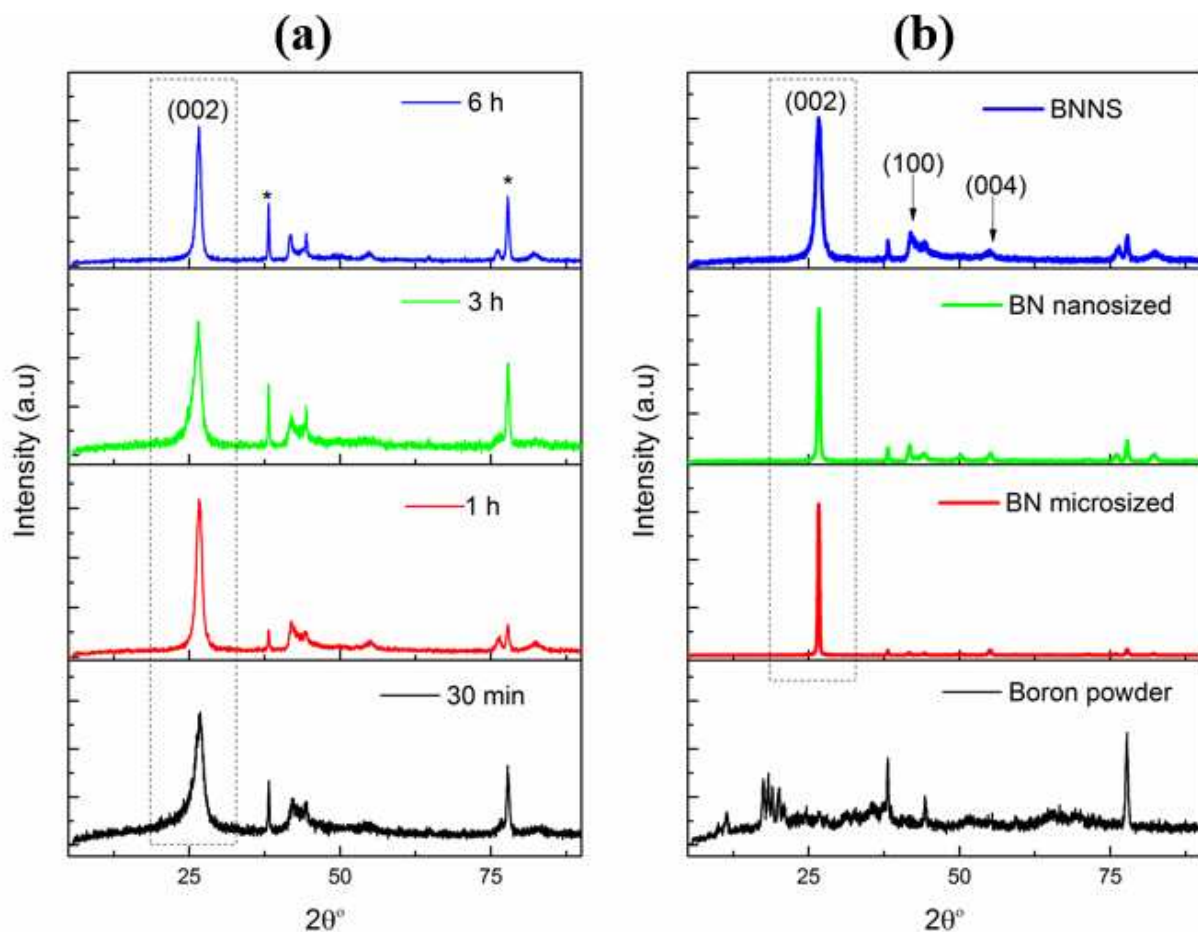


Fig. 3. (a) XRD pattern of BNNS synthesized at 1200 °C for different times (b) comparison between BNNS synthesized at 1200 °C for 1 h, pure boron powder, nano- and micron- sized commercial BN

XRD patterns of BNNS synthesized at 1200 °C for different time intervals (30 min, 1 h, 3 h and 6 h) are shown in Fig. 3(a). XRD patterns of products obtained at varying times are almost similar with a major diffraction peak (002) appears at $2\theta = 26.5^\circ$ confirming successful production (crystallization) of BNNS [45]. However, it is worth mentioning that unlike the product obtained at 1200 °C for 1 h, the products obtained for all other reaction times (for fixed 1200 °C temperature) had unreacted boron as indicated by asterisk in XRD patterns (Fig. 3(a)). It is also peculiar that the thickness of BNNS produced at 1200 °C for different reaction times was almost similar (Table 1). Comparison of XRD patterns of BNNS synthesized at 1200 °C for 1 h, pure boron powder, nano- and micron-sized BN (commercial) are shown in Fig. 3(b). The XRD pattern of our synthesized BNNS is similar to commercial BN. BNNS synthesized in this work has more broadening in (002) peak than commercial BN which clearly suggests formation of

BNNS (Fig. 3(b)). On the basis of XRD analysis, it can be concluded that optimum parameters for the synthesis of BNNS from boron and ammonia reaction are 1200 °C and 1 h. The product yield was found to be 93-97 %, which also indicates that boron powder completely reacted with ammonia resulting in a very high yield of BNNS.

Table 1. Thickness of BNNS synthesized under various conditions determined from XRD analysis.

Sr. No.	Description of BNNS synthesized (temperature and time)	Thickness (nm)
1.	BNNS produced at 900 °C for 1 h	5.20
2.	BNNS produced at 900 °C for 3 h	5.25
3.	BNNS produced at 900 °C for 6 h	5.81
4.	BNNS produced at 900 °C for 9 h	6.01
5.	BNNS produced at 1200 °C for 1 h	11.05
6.	BNNS produced at 1200 °C for 3 h	12.24
7.	BNNS produced at 1200 °C for 6 h	17.14
8.	BNNS produced at 1400 °C for 1 h	15.60
9.	BN nano-sized (commercial)	196

3.2. FTIR

FTIR spectra of commercial nanosized-BN and in-house synthesized BNNS at different temperatures for 1 h reaction time are presented in Fig. 4. In these spectra, two strong characteristic absorption bands at ca. 1350 cm⁻¹ and 760 cm⁻¹ corresponding to sp² bonded B-N and B-N-B bending vibrations, respectively, were observed for all samples [46]. This implies that B-N bond formation occurred at all temperatures studied in this work. However, the products formed at 900 and 1050 °C clearly have some transmittance peaks between 760 and 1350 cm⁻¹ wavenumber due to the formation of initial complexes BNBH and B₂N at 1136 and 902 cm⁻¹, respectively [47], confirming the fact that at these temperatures products formed also accompanied with intermediate B and N complexes [48]. It can be implied from FTIR analysis that initially boron and ammonia reacts to produce various complexes. These complexes

dissociate at temperature higher than 1050 °C leading to crystallization of BN phase. Gross et al. [44] reported that the reaction of urea and boric oxide results in the formation of various intermediate precursors such as ammonium bis(biureto)borate. On the basis of thermogravimetric analysis they found that this complex converts to BN by decomposition at about 850 °C. We determined from FTIR analysis that various boron-ammonia complexes formed for the products synthesized after reaction at 900 and 1050 °C (Fig. 4). However, no such complexes were observed for the products formed after reaction at 1200 °C and 1400 °C, therefore, we believe that product formed at 1200 °C is pure.

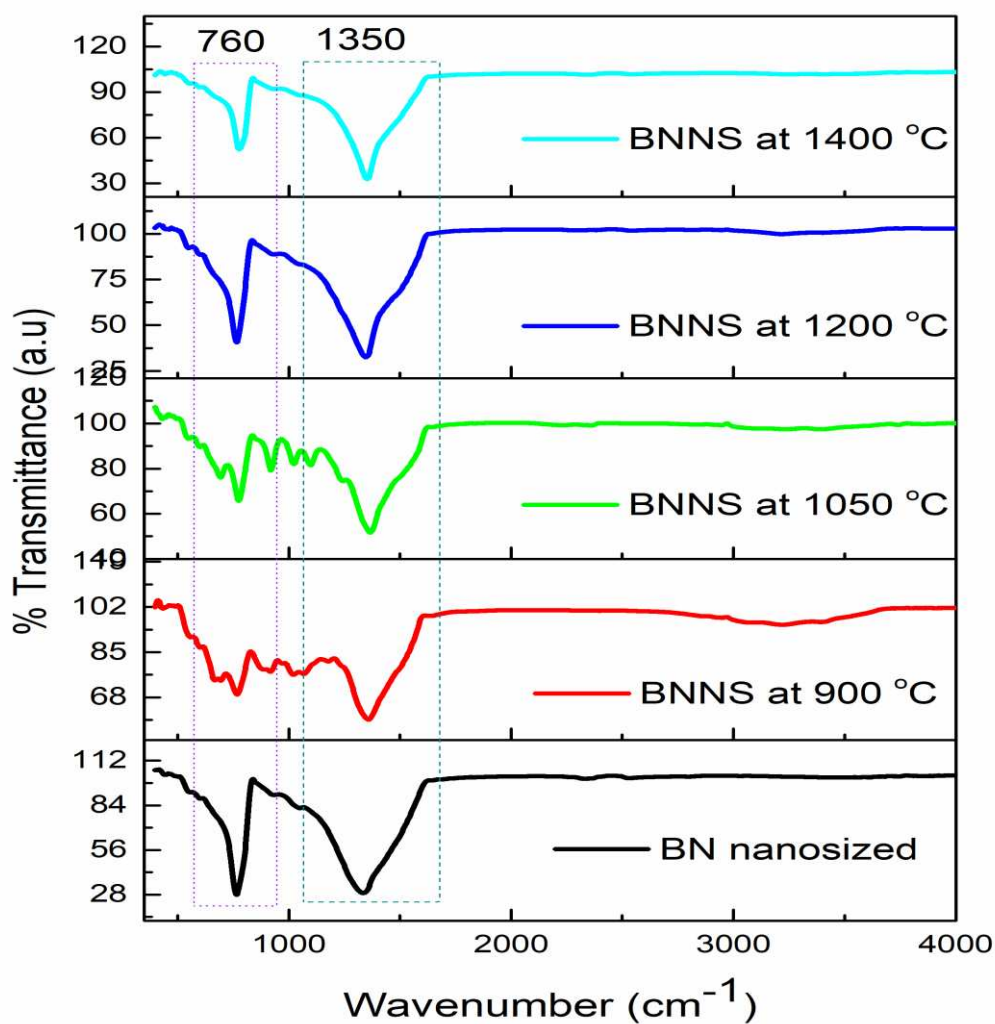


Fig. 4. FTIR spectra of nanosized BN (commercial) and in-house synthesized BNNS at different temperature for 1 h reaction time. The characteristic bands of BN are indicated with rectangles.

3.3. SEM and EDX

SEM images of BNNS synthesized at 900 °C and 1200 °C for 1 h reaction are presented in Fig. 5. The sheet-like morphology of the reaction products can be seen from these images. It should be noted from SEM images of the product obtained at 900 °C (Fig. 5 (a & b)) that the product might have BNBH and B₂N complexes which could be less than 10 % of total product.

SEM images of the product obtained at 1200 °C show that some of the sheets are fused with one another or cohered, which is highly likely due to high temperature involved in the synthesis (Fig. 5(c & d)). The fusion bonding of sheets might have occurred due to melting of some of the boron complexes at higher temperature. The highly polar nature of BN bond could also promote electrostatic bonding between the sheets. Nevertheless, such physical or fusion bonding between sheets can be easily broken by grinding or ultrasonication. Fig. 7 shows AFM images of isolated sheets which were obtained by ultrasonication of BNNS in ethanol.

The layered morphology of the sheets can be clearly seen in the high magnification images (Fig. 5(e & f)). The lateral dimensions of the sheets are in the range of 500 nm to 1 μm. To see the morphology and dimensions of the individual nanosheets, the reaction product was sonicated in ethanol and examined using AFM, which will be discussed in the next section.

EDX analysis of the BNNS synthesized at 1200 °C for 1 h reaction is presented in Fig. 6. Both B and N were detected in the products showing successful synthesis of BNNS. The EDX analysis of commercial nanosized BN is also presented in Fig. 6. Additional peaks around 1.5 keV and 2.2 keV corresponds to aluminum sample stub and gold, respectively.

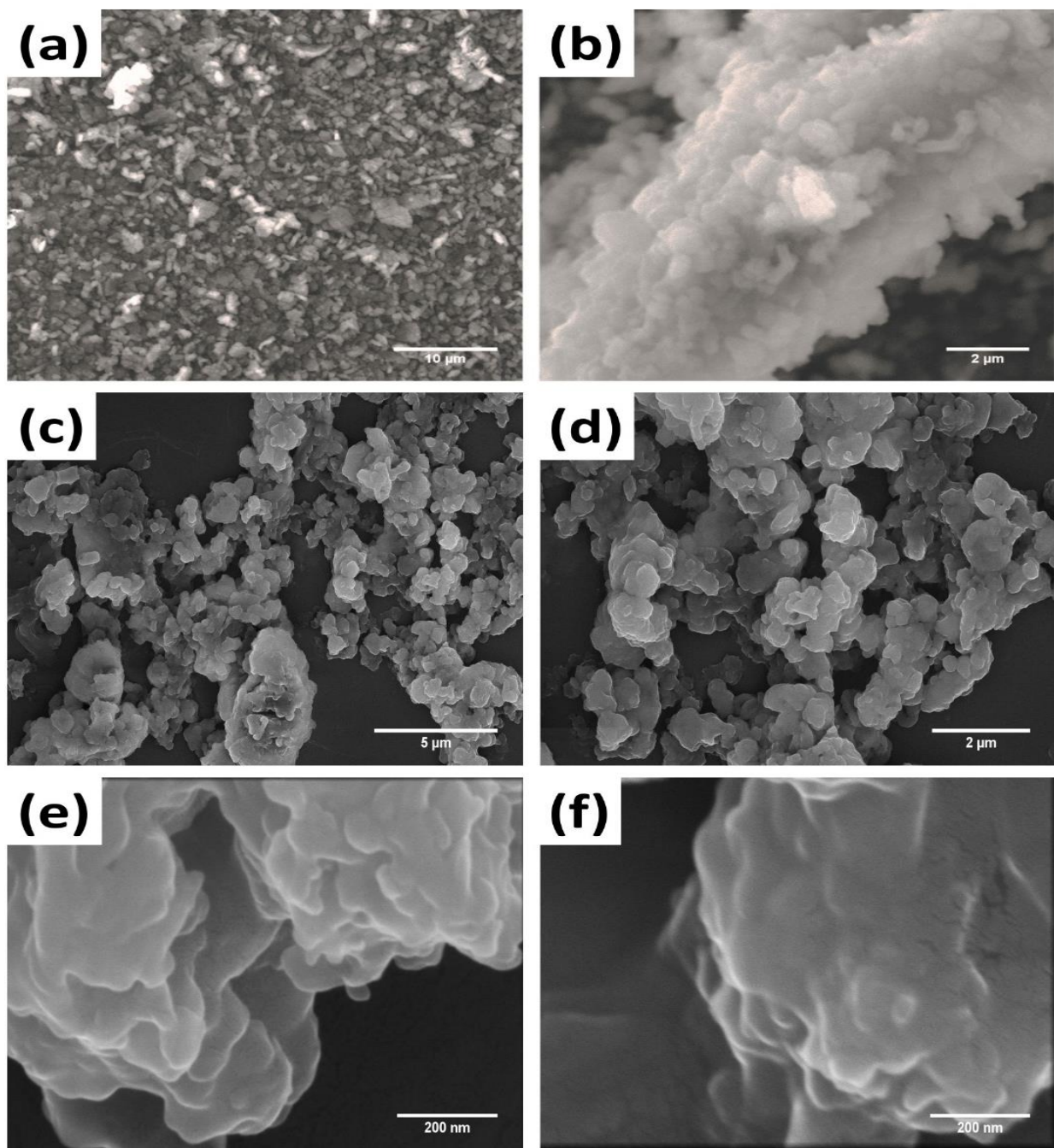


Fig. 5. SEM images of BNNS synthesized at (a & b) 900 °C and (c-f) 1200 °C

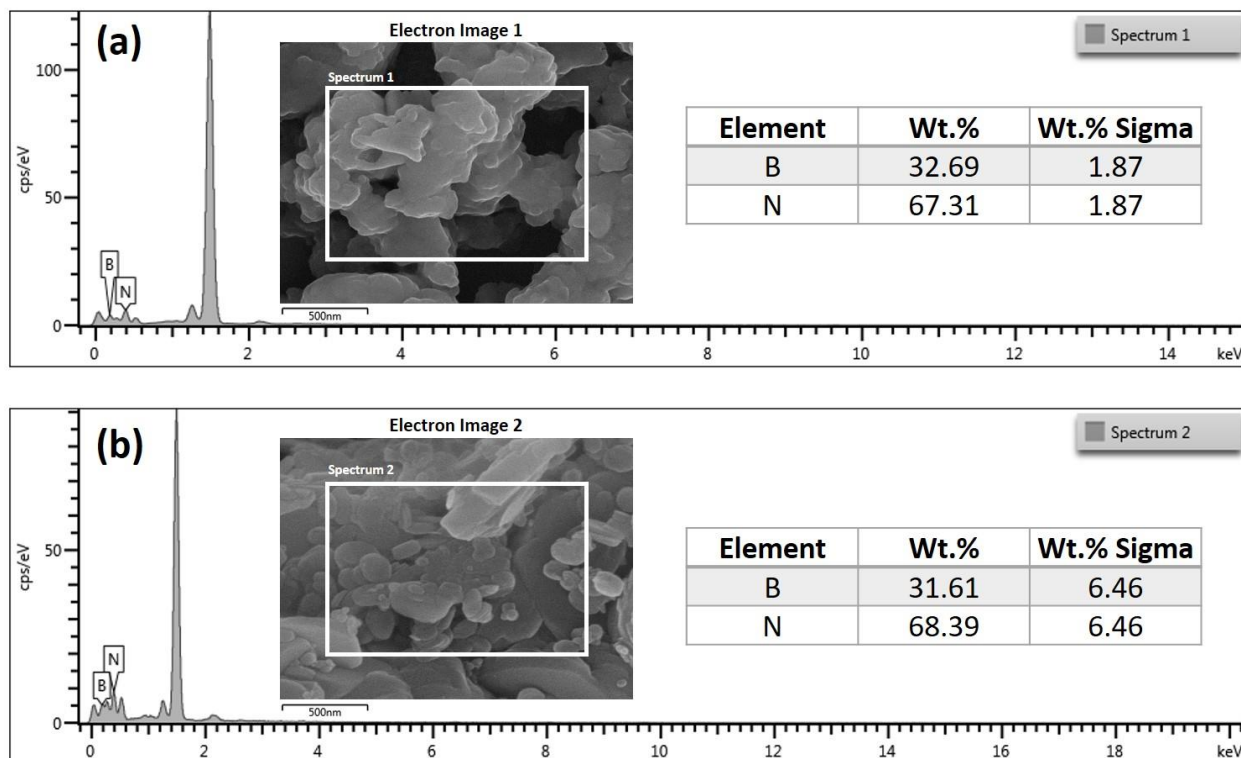


Fig. 6. EDX analysis of (a) BNNS synthesized at 1200 °C (b) commercial BN (nano-sized).

3.4. AFM

Semi-contact mode AFM images of BNNS, with their height profiles, synthesized at 1200 °C for 1 h reaction time are presented in Fig. 7. The sample was prepared by dispersing BNNS in isopropanol alcohol using probe sonication for 1 h. This was necessary to acquire images of individual and isolated sheets, which was successfully done as shown in Fig. 7. The thickness of BNNS was found in the range of 4-8 nm and lateral dimension in the range of 0.5-1 μm . The thickness value is in good agreement with that determined by XRD analysis (Table 1). The higher value obtained through XRD analysis than AFM analysis is because XRD gives an average thickness of large volume of sheets while AFM thickness was obtained from analysis of few nanosheets.

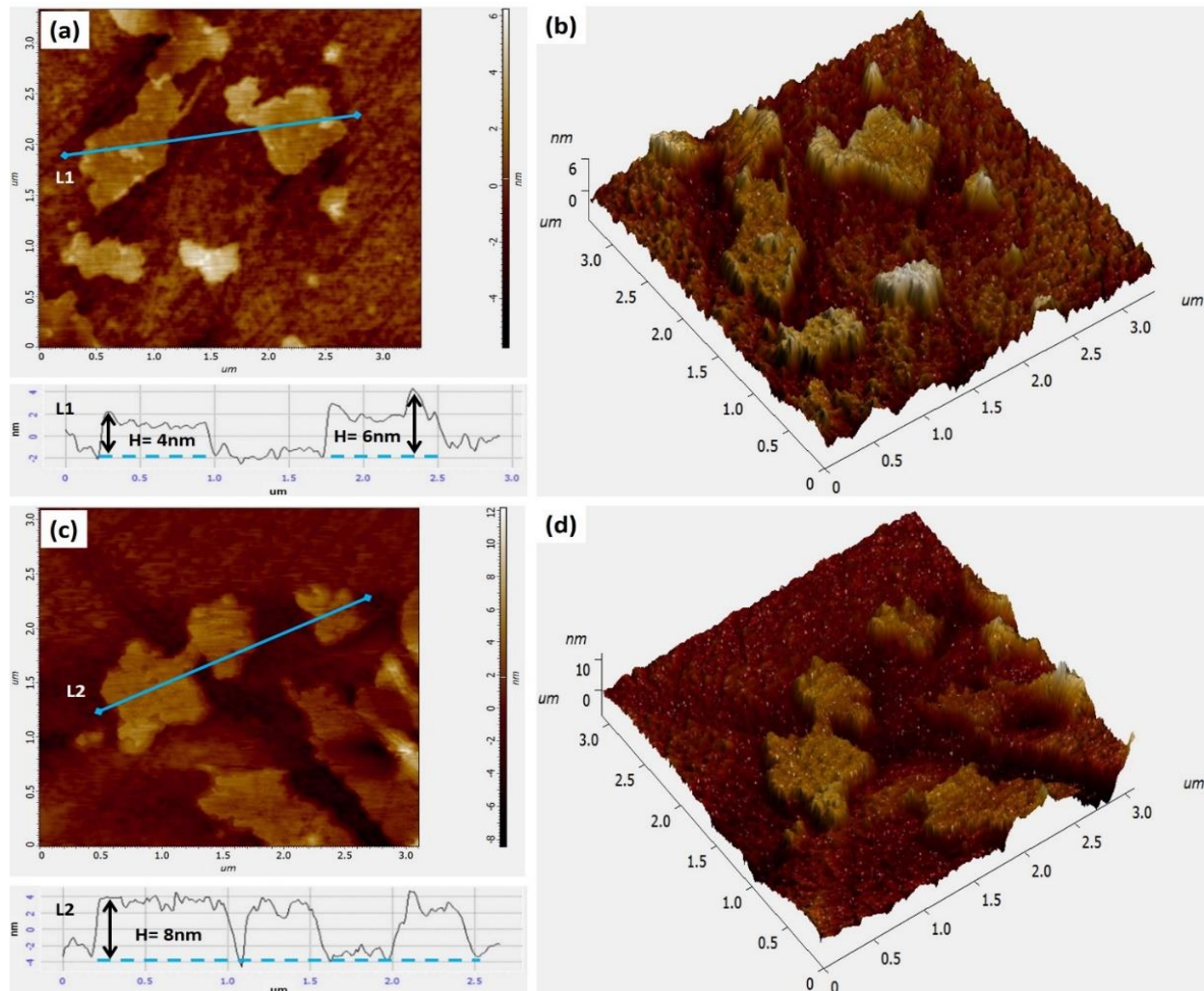


Fig. 7. AFM images with corresponding height profiles (a, c) 2D and (b, d) 3D of BNNS synthesized at 1200 °C for 1 h

3.5. UV-Vis Spectroscopy

UV spectra of nano-sized BN (commercial) and in-house synthesized BNNS (at 1200 °C for 1 h reaction) are presented in Fig. 8. The absorbance for the former and later was found at about 227 and 229 nm, respectively, which is in agreement to that reported in the literature [7]. Band gap of in-house synthesized BNNS as determined from Tauc plot (Fig. 8) was found ca. 5.10 eV and for nanosized BN (commercial) was found to be about 5.11 eV.

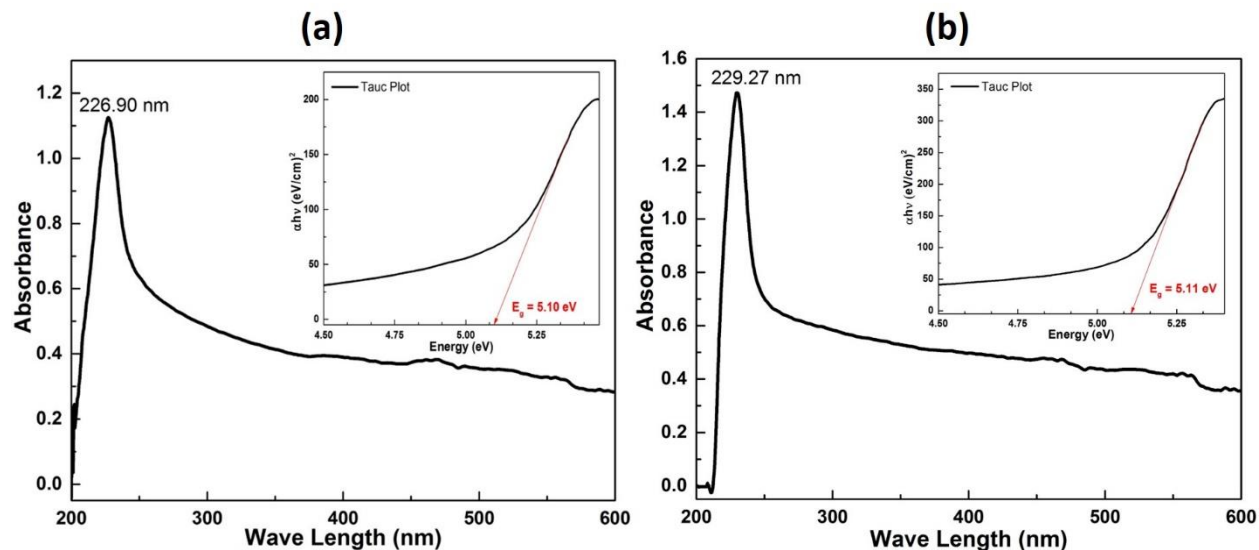


Fig. 8. UV-vis spectrum of (a) BNNS synthesized at 1200 °C for 1 h (b) commercial BN nano-sized

4. Conclusions

After studying both the top down and bottom up approaches of making few layered BNNS, a new approach was used in this work by directly reacting elemental boron precursor with ammonia gas in CVD furnace without the assistance of metal catalyst. The product synthesized through a successive series of experiments which involves variation in temperature (900 to 1400 °C) and time (1 to 9 h). Based on XRD analysis, optimized temperature and time for synthesis of BNNS was found to be 1200 °C and 1 h, respectively. The product yield came out as 93-97% showing almost completion of the reaction. Before and after the narrow range of temperature about 1200 °C, the product yield remained noticeably lower than what it was at 1200 °C, while purity of BNNS phase was compromised. The thickness of BNNS increased from 5 to 11 nm with increase in reaction temperature from 900 to 1200 °C. FTIR analysis revealed two strong characteristic absorption bands at ca. 1350 cm^{-1} and 760 cm^{-1} confirming sp^2 bonded BN and BNB bending vibrations. The morphology and dimensions of the synthesized nanosheets were found convincing by the SEM images. Finally, the thickness of BNNS determined through Scherrer equation and the AFM analysis was found to be ca. 11 and 6 nm, respectively. The novel approach reported in this work may help in commercially producing 5-11 nm thick layered product of BNNS in volume within a moderate cost.

References

1. Novoselov, K.S., et al., *Two-dimensional atomic crystals*. Proceedings of the National Academy of Sciences, 2005. **102**(30): p. 10451-10453.
2. Zhang, Y., et al., *Experimental observation of the quantum Hall effect and Berry's phase in graphene*. nature, 2005. **438**(7065): p. 201.
3. Zeng, H., et al., *"White graphenes": boron nitride nanoribbons via boron nitride nanotube unwrapping*. Nano letters, 2010. **10**(12): p. 5049-5055.
4. Lee, C., et al., *Measurement of the elastic properties and intrinsic strength of monolayer graphene*. science, 2008. **321**(5887): p. 385-388.
5. Balandin, A.A., et al., *Superior thermal conductivity of single-layer graphene*. Nano letters, 2008. **8**(3): p. 902-907.
6. Dean, C.R., et al., *Boron nitride substrates for high-quality graphene electronics*. Nature nanotechnology, 2010. **5**(10): p. 722.
7. Watanabe, K., T. Taniguchi, and H. Kanda, *Direct-bandgap properties and evidence for ultraviolet lasing of hexagonal boron nitride single crystal*. Nature materials, 2004. **3**(6): p. 404.
8. Liu, Y.-R., et al., *Highly Active Pt/BN Catalysts for Propane Combustion: The Roles of Support and Reactant-Induced Evolution of Active Sites*. ACS Catalysis, 2019. **9**(2): p. 1472-1481.
9. Yang, J., et al., *Novel photodriven composite phase change materials with bioinspired modification of BN for solar-thermal energy conversion and storage*. Journal of Materials Chemistry A, 2016. **4**(24): p. 9625-9634.
10. Lin, L., et al., *Synthesis of boron nitride nanosheets with a few atomic layers and their gas-sensing performance*. Ceramics International, 2016. **42**(1): p. 971-975.
11. Sun, N. and Z. Xiao, *Synthesis and performances of phase change materials microcapsules with a polymer/bn/tio2 hybrid shell for thermal energy storage*. Energy & Fuels, 2017. **31**(9): p. 10186-10195.
12. Li, H., et al., *Reduced graphene oxide/boron nitride composite film as a novel binder-free anode for lithium ion batteries with enhanced performances*. Electrochimica Acta, 2015. **166**: p. 197-205.
13. Zhi, C., et al., *Large-scale fabrication of boron nitride nanosheets and their utilization in polymeric composites with improved thermal and mechanical properties*. Advanced Materials, 2009. **21**(28): p. 2889-2893.
14. Nag, A., et al., *Graphene analogues of BN: novel synthesis and properties*. ACS nano, 2010. **4**(3): p. 1539-1544.
15. Golberg, D., et al., *Boron nitride nanotubes and nanosheets*. ACS nano, 2010. **4**(6): p. 2979-2993.
16. Arenal, R., et al., *Young modulus, mechanical and electrical properties of isolated individual and bundled single-walled boron nitride nanotubes*. Nanotechnology, 2011. **22**(26): p. 265704.
17. Song, L., et al., *Large scale growth and characterization of atomic hexagonal boron nitride layers*. Nano letters, 2010. **10**(8): p. 3209-3215.
18. Shen, L., et al., *A long-term corrosion barrier with an insulating boron nitride monolayer*. Journal of Materials Chemistry A, 2016. **4**(14): p. 5044-5050.
19. Jiang, X.-F., et al., *Recent progress on fabrications and applications of boron nitride nanomaterials: a review*. Journal of Materials Science & Technology, 2015. **31**(6): p. 589-598.
20. Park, C.-H. and S.G. Louie, *Energy gaps and stark effect in boron nitride nanoribbons*. Nano letters, 2008. **8**(8): p. 2200-2203.
21. Ouyang, T., et al., *Thermal transport in hexagonal boron nitride nanoribbons*. Nanotechnology, 2010. **21**(24): p. 245701.

22. Raza, M., et al., *Effect of boron nitride addition on properties of vapour grown carbon nanofiber/rubbery epoxy composites for thermal interface applications*. Composites Science and Technology, 2015. **120**: p. 9-16.
23. Li, C., et al., *Thickness-dependent bending modulus of hexagonal boron nitride nanosheets*. Nanotechnology, 2009. **20**(38): p. 385707.
24. Liu, X., et al., *Preparation of polyimide composites reinforced with oxygen doped boron nitride nano-sheet as multifunctional materials*. Materials & Design, 2019. **180**: p. 107963.
25. Pakdel, A., et al., *Low-dimensional boron nitride nanomaterials*. Materials Today, 2012. **15**(6): p. 256-265.
26. Pakdel, A., et al., *Boron nitride nanosheet coatings with controllable water repellency*. Acs Nano, 2011. **5**(8): p. 6507-6515.
27. Jiang, L., et al., *High-resolution characterization of hexagonal boron nitride coatings exposed to aqueous and air oxidative environments*. Nano Research, 2017. **10**(6): p. 2046-2055.
28. Li, L.H., et al., *Boron nitride nanosheets for metal protection*. Advanced materials interfaces, 2014. **1**(8): p. 1300132.
29. Lee, C., et al., *Frictional characteristics of atomically thin sheets*. science, 2010. **328**(5974): p. 76-80.
30. Pacile, D., et al., *The two-dimensional phase of boron nitride: Few-atomic-layer sheets and suspended membranes*. Applied Physics Letters, 2008. **92**(13): p. 133107.
31. Sutter, P., et al., *Chemical vapor deposition and etching of high-quality monolayer hexagonal boron nitride films*. ACS nano, 2011. **5**(9): p. 7303-7309.
32. Meyer, J.C., et al., *Selective sputtering and atomic resolution imaging of atomically thin boron nitride membranes*. Nano letters, 2009. **9**(7): p. 2683-2689.
33. Wang, Y., Z. Shi, and J. Yin, *Boron nitride nanosheets: large-scale exfoliation in methanesulfonic acid and their composites with polybenzimidazole*. Journal of Materials Chemistry, 2011. **21**(30): p. 11371-11377.
34. Marsh, K., M. Souliman, and R.B. Kaner, *Co-solvent exfoliation and suspension of hexagonal boron nitride*. Chemical Communications, 2015. **51**(1): p. 187-190.
35. Thangasamy, P. and M. Sathish, *Supercritical fluid processing: a rapid, one-pot exfoliation process for the production of surfactant-free hexagonal boron nitride nanosheets*. CrystEngComm, 2015. **17**(31): p. 5895-5899.
36. Gao, R., et al., *High-yield synthesis of boron nitride nanosheets with strong ultraviolet cathodoluminescence emission*. The Journal of Physical Chemistry C, 2009. **113**(34): p. 15160-15165.
37. Basu, A. and J. Mukerji, *Synthesis of boron nitride*. Bulletin of Materials Science, 1990. **13**(3): p. 165-171.
38. Ali, S., et al., *Issues associated with the development of transparent oxynitride glasses*. Ceramics International, 2015. **41**(3): p. 3345-3354.
39. Mulfinger, H.O., *Physical and chemical solubility of nitrogen in glass melts*. Journal of the American Ceramic Society, 1966. **49**(9): p. 462-467.
40. Loehman, R.E., *Preparation and properties of oxynitride glasses*. Journal of Non-Crystalline Solids, 1983. **56**(1-3): p. 123-134.
41. Wang, Z.-X., M.-B. Huang, and P. von Rague Schleyer, *Theoretical Study of Boron– Ammonia Reactions*. The Journal of Physical Chemistry A, 1999. **103**(32): p. 6475-6484.
42. Muniz, F.T.L., et al., *The Scherrer equation and the dynamical theory of X-ray diffraction*. Acta Crystallographica Section A: Foundations and Advances, 2016. **72**(3): p. 385-390.

43. Thomas, J., N. Weston, and T. O'connor, *Turbostratic boron nitride, thermal transformation to ordered-layer-lattice boron nitride*. Journal of the American Chemical Society, 1962. **84**(24): p. 4619-4622.
44. Gross, P. and H.A. Höpfe, *Unravelling the urea-route to boron nitride: synthesis and characterization of the crucial reaction intermediate ammonium bis (biureto) borate*. Chemistry of Materials, 2019. **31**(19): p. 8052-8061.
45. Zhang, S., et al., *Ultrathin BN nanosheets with zigzag edge: one-step chemical synthesis, applications in wastewater treatment and preparation of highly thermal-conductive BN-polymer composites*. Journal of Materials Chemistry A, 2013. **1**(16): p. 5105-5112.
46. Du, M., Y. Wu, and X. Hao, *A facile chemical exfoliation method to obtain large size boron nitride nanosheets*. CrystEngComm, 2013. **15**(9): p. 1782-1786.
47. Thompson, C.A., et al., *Infrared spectra of boron-ammonia reaction products in solid argon*. The Journal of Physical Chemistry, 1995. **99**(38): p. 13839-13849.
48. Cui, Z., et al., *Large scale thermal exfoliation and functionalization of boron nitride*. Small, 2014. **10**(12): p. 2352-2355.